

Learning Grasp Configurations for Novel Objects from Prior Examples

Hao Tian¹, Changbo Wang¹, Dinesh Manocha², and Xinyu Zhang^{*1}

¹ School of Computer Science and Software Engineering,
East China Normal University, Shanghai, China
`xyzhang@sei.ecnu.edu.cn`

² Department of Computer Science and Electrical & Computer Engineering,
University of Maryland at College Park, Maryland, USA

Abstract. We present a new approach to learning grasp configurations for a novel object from prior example objects. We assume the novel object and the example object belong to the same category (i.e., objects share the same topologies and have similar shapes). Both the novel and the example objects are segmented into the same semantic parts. We learn a grasp space for each part of the example object using a combination of optimization and learning algorithms. We perform shape warping between the corresponding parts of the example object and the novel object and then compute the corresponding grasps based on the results. Finally, we assemble the individual parts and the associated grasps on the novel object and use local replanning to adjust grasp configurations to satisfy the stability and physical constraints (e.g., that the grasp are penetration-free). Our algorithm can automatically handle a wide range of object categories and a variety of robotic hand grasps.

Keywords: Manipulation & Grasping, Grasp Space, Grasp Planning, Grasp Transfer

1 Introduction

Robot grasping has a wide range of applications in industrial automation and humanoid service robots. Given an object, the goal of grasping is first to compute feasible and stable grasps and then to execute grasping tasks using a gripper or a multi-fingered robotic hand. Many techniques have been proposed to interpret, compute, or evaluate grasps and their stability. These techniques can be broadly categorized into physically-based approaches and data-driven approaches. Physically-based approaches (or analytic approaches) take into account the laws of physics and address the problems of contact computation, force-closure, grasp feasibility, grasp stability [3, 14, 16, 30], etc. Data-driven approaches (or empirical approaches) gather grasping knowledge by sampling grasp configurations in virtual simulations or recording how a real robot or even a human performs grasping tasks [5, 13, 18, 34, 43]. Recently, machine learning techniques have also been used for planning robust grasps [25, 28, 29].

Some data-driven approaches aim to construct a grasp database for various models by computing a set of stable grasp configurations for each object. However, it is very computationally expensive to compute stable grasp spaces when many new objects are added to the grasp database. Therefore, some techniques have been proposed to transfer or reuse the grasps between objects of similar shapes [7, 18, 20, 26, 40, 41], as opposed to computing stable grasps for the novel objects from scratch. These works mimic the way that humans learn grasping behaviors based on object categories that group objects with similar topologies and geometric shapes [1]. Moreover, studies in neuro-psychology for object manipulation indicate that, when humans perceive an object to grasp, the object is parsed into a few constituent parts with different affordances [4, 21]. Some parts of an object are designed to be suitable for grasping. For instance, a handle of a mug is designed for grasping. Such a parsing process corresponds to segmenting an object into different semantic and functional parts. To perform good grasps, the key is to find a suitable part of the given object for grasping.

Main Results: In this paper, we present a new approach to learning grasp configurations for a novel object from prior example objects. We assume the novel object and the example object belong to the same category in which objects share the same topologies and have similar shapes [37, 41]. We compute a grasp space for each part of the example object using a combination of learning and optimization algorithms. For a novel object with the same category, we segment the object into parts and compute a shape warping function between the corresponding parts of the example object and the novel object. The contact points of a given grasp on the example object are mapped to the novel objects through a shape warping function and then the corresponding grasps for each part of the novel object are determined. Finally, we assemble the individual parts and their corresponding grasps and use local replanning to adjust grasp configurations to ensure the stability and physical constraints (e.g., that they are penetration-free) of the overall grasp of the novel objects. We test our algorithm with three categories: mug, spray bottle, and power drill. These models are non-symmetric, non-convex, and have different affordances. These characteristics make grasping objects very challenging. In our experiments, we use a three-fingered Barrett hand to grasp objects. Our method has a high success rate of learning grasp configurations for novel objects and exhibits better performance than some previous work.

The rest of the paper is organized as follows. In Section 2, we briefly present prior work on object grasping with similar characteristics. In Section 3, we give the overview of our approach. We describe the process of computing the grasp spaces for segmented parts using machine learning and optimization techniques in Section 4. Section 5 presents our overall algorithm for grasp transfer, including shape warping, contact warping, local replanning, and part assembly. We provide implementation and experimentation results and comparison in Section 6.

2 Related Work

In this section, we give a brief overview of prior work on object grasping, especially grasp transfer and part-based grasping.

Grasping Similar Objects: These techniques rely on the fact that objects can be grouped into categories with common characteristics, such as usage, application, or geometric shape. Such categories must be known for grasping tasks. Nikandrova et al. [33] demonstrated a category-based approach for object grasping. Different methods have been proposed to determine the object categories automatically [27, 31] and define an object representation and a similarity metric for grasp transfer [5]. For a novel object, a known similar object and its preplanned grasps were retrieved from a grasp database [18, 26]. Li et al. [26] proposed a shape matching algorithm for grasping based on relative placements and surface normals. Curtis et al. [12] used Gaussian distributions to define basic shape features. Grasp planning accumulates knowledge gained from prior grasping actions and efficiently creates a proper grasp for a novel object. Geometric proximity was also used to find similar objects in a predefined grasp database [18].

Grasp Transfer: Shape similarity has been used to transfer grasps to novel objects [7, 18, 26]. Vahrenkamp et al. [41] transferred grasp poses according to their shape and local volumetric information. Grasp transfer was used to preserve the functionality of pre-planned grasps using surface warping [20]. In [2, 40], grasp poses were transferred using a contact warp method suggested in [19]. This method minimized the distance between the assigned correspondences. The warped contacts were locally replanned to ensure grasp stability. Diego et al. [38] transferred manipulation skills to novel objects using a non-rigid registration method. This work was extended by accumulating grasping knowledge and shape information [37]. In [24], probability densities were learned to model a demonstrated grasp [24]. The method did not require knowledge about an object’s category when performing grasp transfer.

Part-based Grasping: Many techniques have been proposed to segment objects into parts and perform grasp planning on the resulting parts. In [17, 22], objects were represented with simplified data structures such as superquadric and minimum volume bounding boxes to reduce the complexity of planning grasps. Aleotti et al. [1] proposed an approach based on programming by demonstration and 3D shape segmentation. Their shape segmentation was based on Reeb graphs that were used to generate a topological representation of the objects.

3 Overview

3.1 Problem Definition and Notations

Given an example object and a novel object, our goal is first to compute the grasp space for the segmented example object and transfer that knowledge to a novel object. We assume that the example object and the novel object belong to the same category. Here, a category is composed of a set of objects which

share the same topology and have a similar geometric shape. Objects can be categorized depending on different criteria such as object shape, object topology, or application. Therefore, in this paper, we assume that the example object and the novel object can be segmented into parts that have the same topology and a similar geometric shape.

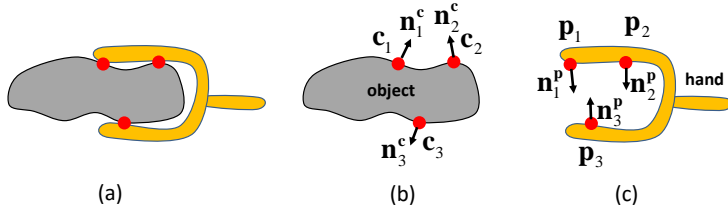


Fig. 1. Grasp configuration and contacts. (a) A grasp configuration. (b) Contacts on the object surface corresponding to a grasp. (c) The pre-defined points on the hand.

Assume that a multi-fingered hand consists of k joints and the joint variables are $\Theta = \{\theta_1, \theta_2, \dots, \theta_k\}$. Due to the high number of finger joints, the grasp space is typically a high-dimensional space, which is a subset of the configuration space constructed using a multi-fingered hand and an object to be grasped. A grasp space corresponds to a set of stable grasp configurations at which an object can be firmly grasped. To grasp an object, a multi-fingered robotic hand must have multiple contacts with the object. As shown in Figure 1, a grasp configuration corresponds to a few contacts between the hand (orange) and the object (grey). The contacts on the object surface is denoted by \mathbf{c} and its normal are denoted by \mathbf{n}_i^c . The predefined points on the hand is denoted by \mathbf{p} and its normal is denoted by \mathbf{n}_i^p .

3.2 Algorithm Overview

Figure 2 gives the overview of our algorithm. For an example object to be grasped using a given robotic hand, we first obtain its semantic segmentation and then compute the grasp space for each segment. Here, we use a support vector machine (SVM) to compute an initial approximation of the configuration space for each segment part. Then, we refine the grasp space using particle swarm optimization. Next, we transfer the grasp space of the example object to other novel objects. Since we assume that both the example object and the novel object belong to the same category, the novel object can be segmented into parts in the same way as the example object. We compute shape warping between the corresponding parts of the example object and the novel object. The contact points are first mapped to the novel object using shape warping and then its feasible grasp configuration is determined. Finally, we assemble individual parts of the novel object and use local replanning to adjust grasp configurations to ensure the stability and physical constraints of the resulting grasps.

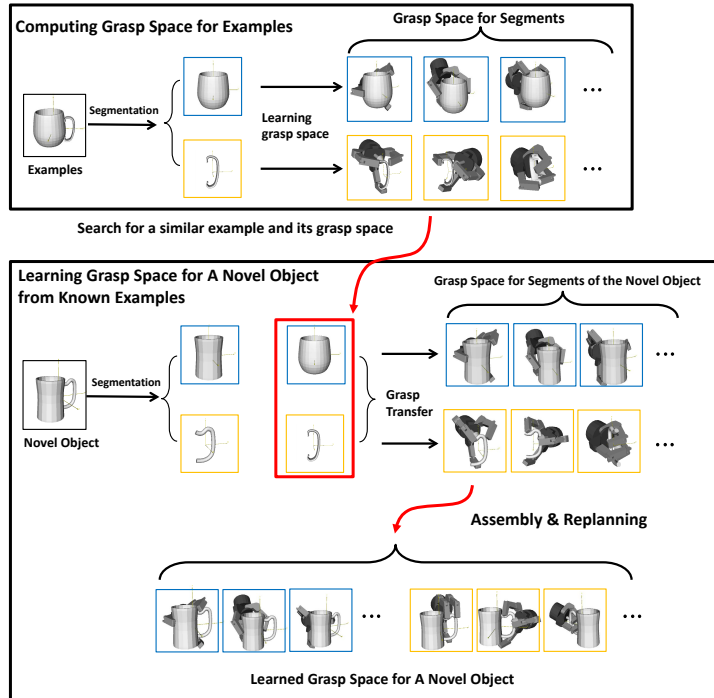


Fig. 2. Learning grasp configurations for a novel object from prior examples. We assume that the example object and the novel object belong to the same category and that they have been segmented into parts. Top: Computing stable grasp space (a set of stable grasp configurations) for a given prior example. Bottom: Learning a stable grasp space (a set of stable grasp configurations) for a novel object from the prior example. Our algorithm consists of the following stages: object segmentation, grasp transfer, part assembly and grasp replanning.

4 Learning Grasp Space for Examples

Given an example object to be grasped, we first segment it into semantic parts. Next, we compute an approximation of the grasp space for each part. To approximate the grasp space, we first randomly sample the configuration space and compute the collision state for each sample configuration using a discrete collision detection algorithm. There are two possible collision states: in-collision or collision-free, which correspond to a scenario in which the robotic hand collides with the object and a scenario in which it doesn't, respectively. Given a set of samples, we use an SVM technique to train a binary classifier to approximate the configuration space and the resulting decision boundary separates all in-collision configurations from the collision-free configurations.

Our goal is to compute a grasp space for each individual part of the prior example object. The discovery of a stable grasp configuration starting from a ran-

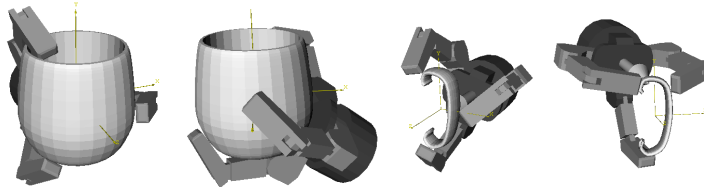


Fig. 3. Learning grasp space for each part of a known example object. Our algorithm is based on support vector machine and particle swarm optimization.

dom configuration in the configuration space can be formulated as an optimization problem. We define the following *energy function* to model the shape fitting and grasping stability between a hand posture and an object to be grasped. Suppose we have a set of pre-specified points on the hand [9]. The energy function is formulated as

$$\sum_i \sum_j (\omega_1 \|\mathbf{p}_i - \mathbf{c}_j\| + \omega_2 (1 - \mathbf{n}_i^{\mathbf{P}} \cdot \frac{\mathbf{p}_i - \mathbf{c}_j}{\|\mathbf{p}_i - \mathbf{c}_j\|})) + \omega_3 \log \epsilon^{-1}, \quad (1)$$

where the first term $\|\mathbf{p}_i - \mathbf{c}_j\|$ is the distance between the i th pre-defined point \mathbf{p}_i on the hand and its corresponding closest point \mathbf{c}_j on the object surface. The second term is based on the angle between the surface normal $\mathbf{n}_i^{\mathbf{P}}$ at \mathbf{p}_i and the vector from \mathbf{p}_i to \mathbf{c}_j . The last term relates to grasp quality [15] and $\epsilon \in (0, 1]$ when the grasp is stable. A small ϵ indicates a relatively small external disturbance that can break a grasp’s stability. ω_1 , ω_2 , and ω_3 are the weights for the three terms, respectively.

We minimize the energy function with respect to the hand pose and joint variables Θ using *particle swarm optimization* [11] and then determine the stable grasps on the example object. This formulation is highly non-linear [35] and small changes in either hand position or finger postures can drastically alter the quality of the resulting grasp. The stochastic nature of particle swarm optimization makes it a particularly good choice for solving the problem. Since a new configuration used in particle swarm optimization is generated as a neighbor of the current configuration, we can avoid collisions during the sampling process. In addition, the computation of an energy gradient is unnecessary and therefore the particle swarm optimization algorithm is particularly applicable to non-linear functions in Equation 1. We treat collision-free support vectors generated from the learning stage as the initial particles with an energy value. Given random searching velocities at the beginning of the optimization algorithm, the particles are updated in an iterative manner based on their velocities. The particle swarm optimization algorithm records the global best position among all the particles and the local best position for each particle. The particle’s movement is influenced by its local best position and the global best position. As a result, every particle is expected to move towards its best position, w.r.t. the given energy function, and the sparsely distributed particles can fully explore configuration space. When particles explore the configuration space, the hand

may collide with the object or have self-collisions between fingers. We use continuous collision detection [36] to compute the first instance of contact that avoids collisions.

When a feasible grasp configuration is obtained, the force closure (FC) can be determined using the contacts between the fingers and the object. The grasp quality is then computed, which is related to the third term in Equation 1. If a grasp configuration is stable, we keep it in the grasp space. As a result, each grasp space is approximated by a set of discrete stable grasp configurations. For an example object consisting of semantic parts, we compute the grasp spaces (i.e. a set of discrete stable grasp configurations) for all the individual parts.

5 Transferring Grasp Space

In this section, we first present our shape warping algorithm for transferring grasp contact points from the segmented parts of a known example object to a novel object. Then we use a grasp transfer and local replanning algorithm to obtain feasible and stable grasps for each part of the novel object.

5.1 Mapping Contacts using Shape Warping

Given a segmented part of an example object and a segmented part of a novel object, two sets of 3D points are uniformly sampled from the surfaces of the two objects. Let $\mathbf{A} = \{\mathbf{a} : \mathbf{a} \in \mathbb{R}^3\}$ be a set of points on the example object and let $\mathbf{B} = \{\mathbf{b} : \mathbf{b} \in \mathbb{R}^3\}$ be a set of points on the novel object. Assuming the two sets have the same number of points, the goal of shape warping is to find the correspondences between \mathbf{A} and \mathbf{B} .

First, we compute a rigid alignment, a transformation from \mathbf{A} to \mathbf{B} , to match the corresponding parts of the two objects. The resulting rigid alignment will be able to tolerate shape deviations between the example shape and the novel shape. The transformation ($\mathbf{R} \in SO(3), \mathbf{T} \in \mathbb{R}^3$) between the two objects is computed by minimizing the deviations:

$$\arg \min_{(\mathbf{R}^*, \mathbf{T}^*)} \sum_{\mathbf{a} \in \mathbf{A}} \|\mathbf{R}\mathbf{a} + \mathbf{T} - \mathbf{b}_a\|^2 + \arccos^2\left(\frac{\mathbf{n}^{\mathbf{b}_a}}{\|\mathbf{n}^{\mathbf{b}_a}\|} \cdot \mathbf{R} \frac{\mathbf{n}^{\mathbf{a}}}{\|\mathbf{n}^{\mathbf{a}}\|}\right), \quad (2)$$

where \mathbf{b}_a is the nearest neighbor point of \mathbf{a} in \mathbf{B} and $\mathbf{n}^{\mathbf{a}}$ and $\mathbf{n}^{\mathbf{b}_a}$ are the normal of \mathbf{a} and \mathbf{b}_a , respectively. After solving this optimization problem, we obtain the transformation of the rigid alignment \mathbf{R}^* and \mathbf{T}^* .

Second, we determine the correspondences between the two sets of points \mathbf{A} and \mathbf{B} . Here, we use the correspondence mapping method proposed in [19]. Since the rigid alignment between \mathbf{A} and \mathbf{B} has moved the corresponding points very close to one another, we further refine these correspondences using local surface details such as point proximity and normal vectors. In addition, we use both forward correspondence and backward correspondence, defined as follows.

Forward Correspondence: We define a subset of points $\mathbf{B}_\delta = \{\mathbf{b} \in \mathbf{B} | \mathbf{n}^{\mathbf{b}} \cdot \mathbf{R}^* \mathbf{n}^{\mathbf{a}} > \cos \delta\}$. Any point in \mathbf{B}_δ can find the corresponding point in \mathbf{A} and the two points have at most an angle bias δ between their normal vectors. The forward correspondence of point $\mathbf{a} \in \mathbf{A}$ is defined as

$$F(\mathbf{a}) = \arg \min_{\mathbf{b} \in \mathbf{B}_\delta} \|\mathbf{R}^* \mathbf{a} + \mathbf{T}^* - \mathbf{b}\|. \quad (3)$$

Backward Correspondence: Analogously, we define a subset of points $\mathbf{A}_\delta = \{\mathbf{a} \in \mathbf{A} | \mathbf{n}^{\mathbf{a}} \cdot \mathbf{R}^* \mathbf{n}^{\mathbf{b}} > \cos \delta\}$ and define the backward correspondence of point $\mathbf{b} \in \mathbf{B}$

$$F^{-1}(\mathbf{b}) = \arg \min_{\mathbf{a} \in \mathbf{A}_\delta} \|\mathbf{R}^* \mathbf{a} + \mathbf{T}^* - \mathbf{b}\|. \quad (4)$$

We set $\delta = \frac{1}{6}\pi$ for the angle bias between two normal vectors. Using both the forward and backward correspondences, we can determine a correspondence relationship between the two sets of points \mathbf{A} and \mathbf{B} .

Third, we compute a mapping from the domain of \mathbf{A} to the domain of \mathbf{B} using the interpolation of the point correspondences. For any point \mathbf{x} on the example object, we search \mathbf{A} for a subset of nearest points. We denote the subset as \mathbf{A}_x . The forward map of this point \mathbf{x} on the novel object is computed using the average of the forward correspondences of the closest points \mathbf{A}_x . The forward mapping of \mathbf{x} is

$$F(\mathbf{x}) = \frac{1}{\|\mathbf{A}_x\|} \sum_{\mathbf{a} \in \mathbf{A}_x} F(\mathbf{a}), \quad (5)$$

where $\|\mathbf{A}_x\|$ is the number of elements in \mathbf{A}_x . Analogously, we compute a backward mapping for a point \mathbf{y} on the novel object as

$$F^{-1}(\mathbf{y}) = \frac{1}{\|\mathbf{B}_y\|} \sum_{\mathbf{b} \in \mathbf{B}_y} F^{-1}(\mathbf{b}), \quad (6)$$

where $\mathbf{B}_y \subset \mathbf{B}$ and it is the set of nearest neighbors of \mathbf{y} .

Finally, we use a forward-backward consistency check of these mappings to ensure the symmetry of the interpolated correspondences. For a point \mathbf{x} on the example object, its forward-backward mapping is $F^{-1}(F(\mathbf{x}))$. We use the following condition to perform forward-backward consistency checking

$$\|\mathbf{x} - F^{-1}(F(\mathbf{x}))\| < \gamma, \quad (7)$$

where γ is a user-specified tolerance and is related to the object dimension. If both the forward and backward mappings pass the consistency check, we can use the forward mapping to warp the grasp contact points to the points on the novel object. Figure 4 shows some warping examples. The left column includes the given example objects. The right two columns include the novel objects, where colored balls indicate the corresponding contact points. The contacts between the robotic hand and the given example object are mapped to the novel objects using shape warping.

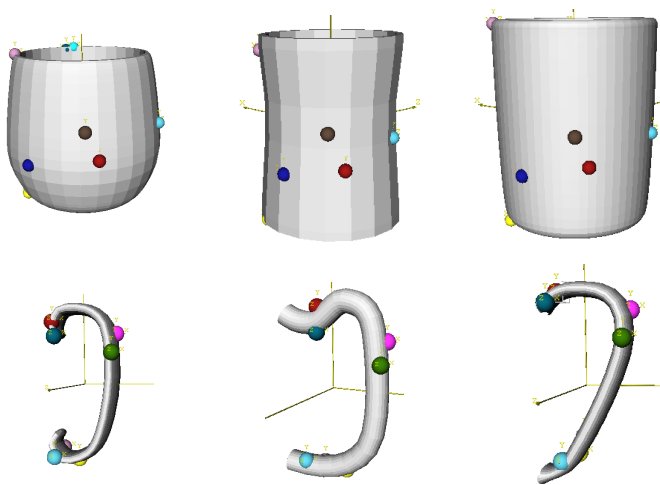


Fig. 4. Mapping contacts using shape warping. The top and bottom rows are segmented parts of the objects. The contacts on the given example objects (left column) are mapped to the novel objects (right two columns) using shape warping.

5.2 Local Replanning for Feasible Grasps

When we directly apply a grasp configuration and the corresponding contacts of the example object to a novel object, it is very likely that there are slight penetrations between the multi-fingered hand and the novel object or that the grasp is not physically stable. Therefore, we use a local replanning technique to generate a stable grasp. We first adjust the joint variables of the hand so that both the variables and the grasp are applicable to the novel object.

Let a finger’s contact position be \mathbf{c} and the warped point on the novel object be \mathbf{d} . We use the following conditions to generate a new grasp:

$$\mathbf{c}_i = \mathbf{d}_i, \quad (8)$$

$$\mathbf{n}_i^{\mathbf{c}} \cdot \mathbf{n}_i^{\mathbf{d}} = -1, \quad (9)$$

where $\mathbf{n}_i^{\mathbf{c}}$ and $\mathbf{n}_i^{\mathbf{d}}$ are the normal vectors of contact points \mathbf{c}_i and \mathbf{d}_i , respectively. The first condition ensures that the pair of corresponding contact points (i.e. the one on the fingers and the other on the object) match in terms of the position. The second condition ensures they have an opposite normal direction. In addition, we limit the range of the joint variable to avoid large finger motions.

$$\theta_i^{low} \leq \theta_i \leq \theta_i^{up}, \quad (10)$$

where θ_i^{low} and θ_i^{up} are the lower and upper bounds of the i th joint θ_i , respectively. Using the objective function [6] given in Equation 11 subject to the above

constraints, we obtain a grasp by solving for the joint variables Θ^* .

$$\arg \min_{\Theta^*} \sum_i (\omega_4 \|\mathbf{c}_i(\Theta) - \mathbf{d}_i\|^2 + e^{\omega_5(\mathbf{n}_i^c(\Theta) \cdot \mathbf{n}_i^d)}) + \sum_k (e^{\omega_6(-\theta_k + \theta_k^{low})} + e^{\omega_6(\theta_k - \theta_k^{up})}) + \omega_7 \log \epsilon^{-1}, \quad (11)$$

where ω_4 , ω_5 , ω_6 and ω_7 are the weights for contact points, normals, joint angles, and grasp quality, respectively. The first term accounts for the distance between finger contacts $\mathbf{c}_i(\Theta)$ and warped contacts \mathbf{d}_i on the novel object. The second term computes their normal bias. The third term limits a joint’s movement within a given interval. The last term is relevant to grasp quality ϵ . If the objective function converges and yields a set of joint variables Θ^* , a stable grasp is obtained for the novel object.

To solve Equation 11, we use a simulated annealing algorithm [23] to explore the configuration space and search for a stable grasp. The simulated annealing algorithm starts from the best grasp configuration that is initialized with the grasp learned for the example object. In each iteration, we sample the configuration space around the best grasp configuration and check the collision state for each sample. If the sample is in-collision, we explore the configuration space and add more samples (e.g., adding 20 samples at a time). If the new samples are still in-collision, we discard it and proceed to the next iteration. If the sample is collision-free and has a better function value than the current best configuration, we replace the best configuration with this sample. The process proceeds in an iterative manner to find a best configuration. For any collision-free sample, we close the fingers, hold the object and compute its grasping quality using the algorithm described in [15]. If it is stable, we store it as a candidate grasp and repeat the iteration. If the local replanning algorithm terminates, we check the stability of the final grasp. If it is stable, the grasp transfer and local replanning succeed. If the final sample is unstable, we find a stable grasp with the best objective function value from the candidate grasps. If no stable grasps can be found, the grasp transfer fails. Figure 5 shows a few results after grasp transfer and local replanning.

5.3 Grasp Assembling and Replanning

Since the grasp configurations are computed for each part of the novel object, we need to assemble all the individual parts using their original semantic segmentation. We collect a set of grasps resulting from each part. However, these resulting grasps may not be stable for the assembled object or might result in collisions between the fingers and the object. Therefore, we first examine whether a grasp causes any collisions between the hand and the novel object. If any collisions occur between the palm of the hand and the object, we discard the grasp. Note that it is non-trivial to adjust the position of the palm to generate a stable grasp since a slight adjustment may cause significant changes to the fingers. If a grasp results in collisions between a finger and the object, or if a grasp is collision-free

but unstable, we use the replanning algorithm introduced in Section 5.2 to make adjustments and to generate a stable grasp configuration. Figure 6 shows some grasp configurations before and after part assembly and local replanning. Refer to Figure 8 for more results.

6 Experimental Results

In this section, we present our benchmark models, some details about the implementation, and the performance of our algorithm on various objects.

6.1 Benchmark Objects

We evaluated the performance of our algorithm on three categories of objects using a wide variety of grasps. We used a three-fingered Barrett hand to grasp objects. The categories of the benchmark objects include mug, spray bottle, and power drill. In our experiments, we chose one object in each category as an example object and the other two as novel objects. We compute grasp configurations for the segmented parts of each example object and then transfer the grasps to the novel objects. As shown in Figure 7, the leftmost object in each row is selected as the example object.

6.2 Implementation

We implement our transfer algorithm using the GraspIt! library [32]. We use a shape diameter function (SDF) [39] to segment the given objects into parts. The performance is measured using a single thread on a PC with a 3.4GHz Intel i7 CPU and 8GB memory.

When computing the grasp space for each segmented part of the example object, we set $\omega_1 = 0.02$ and $\omega_2 = 1.0$, as suggested in [10]. In addition, we set $\omega_3 = 20$. We sampled 40,000 training data as the input of SVM to learn grasp spaces for all the example objects. We chose collision-free support vectors in SVM as particles during the particle swarm optimization process. The time require to learn the configuration space, the time to compute the grasp space and the number of stable grasps are shown in Table 1.

During grasp transfer, we set $\omega_4 = 10$, $\omega_5 = 5$, $\omega_6 = 5$, and $\omega_7 = 20$ in Equation 11. Table 2 shows the average time of transferring a stable grasp from an example object to the novel object.

6.3 Performance Analysis and Comparisons

We measure grasp quality and grasp transfer success rates to evaluate the performance of our algorithm.

Grasp Quality: We examine the grasp quality for novel objects against grasp quality for example objects. As shown in Figures 9, 10, and 11, we use scatter plots to show the grasp quality. The horizontal and vertical axes represent

example objects	tris	learning contact space (s)	computing stable grasps (s)	# stable grasps
mug body	1864	1343.6	1405.5	133
mug handle	1586	1254.8	1287.1	60
spray bottle body	1844	1404.5	1536.4	194
spray bottle head	894	1286.7	132.8	48
power drill body	4893	1654.2	1604.2	61
power drill head	5052	1795.1	1635.9	56

Table 1. The time to learn the contact space, the time to compute stable grasps, and the number of stable grasps.

novel objects	tris	transfer stage (s)	assembly stage (s)
#1 mug body	752	322.5	305.3
#1 mug handle	1284	294.7	302.5
#2 mug body	2550	335.3	289.2
#2 mug handle	1586	283.1	295.8
#1 spray bottle body	2294	329.0	293.4
#1 spray bottle head	1241	298.9	345.6
#2 spray bottle body	2074	334.4	315.1
#2 spray bottle head	737	312.8	364.2
#1 power drill body	6105	414.7	475.6
#1 power drill head	6850	437.5	498.1
#2 power drill body	6914	421.5	480.5
#2 power drill head	6781	453.4	509.4

Table 2. The average time of grasp transfer and grasp assembly.

the grasp quality for example objects and novel objects, respectively. We show the grasp quality both before part assembly (blue points) and after part assembly/replanning (red).

We also compare our method with a straightforward method that first straightens the colliding fingers and the encloses the object. This method does not use local replanning. Figures 12, 13, and 14 show grasp qualities of our algorithm and the straightforward method. If the difference in grasp quality between the two methods is greater than 0, our grasp is better than the straightforward method. Otherwise, the straightforward method is better than ours. As shown in Figures 12, 13 and 14, because most points distribute above the horizontal axes, our method outperforms the straightforward method. Since our method must match warped contact points, it may influence the final grasp quality and therefore some points distribute below the horizontal axes. We show the grasp quality comparison both before part assembly (blue points) and after part assembly/replanning (red).

Grasp Transfer Success Rate: In this experiment, we transfer 40 grasps from an example object to a novel objects in each scenario. We count the number of successful grasp transfers (i.e. a grasp of the example object is successfully trans-

novel objects	grasp transfer	grasp assembly
#1 mug body	37/35	35/29
#1 mug handle	33/21	29/19
#2 mug body	36/35	36/33
#2 mug handle	33/23	26/29
#1 spray bottle body	36/29	35/29
#1 spray bottle head	32/17	22/14
#2 spray bottle body	34/22	32/19
#2 spray bottle head	28/15	23/18
#1 power drill body	35/17	32/25
#1 power drill head	37/24	33/26
#2 power drill body	39/22	36/26
#2 power drill head	35/20	31/13

Table 3. The number of success in grasp transfer and in grasp assembly. Our method vs. the straightforward method. We transfer 40 grasps from an example object to a novel objects for each scenario. Our method exhibits very high success ratios and outperforms the straightforward method.

ferred to the novel object and the resulting grasp is also stable). We measure the grasp transfer success rate for the two stages: grasp transfer and part/grasp assembly, as shown in Table 3. We also compare our method with the straightforward method. As shown in Table 3, our method exhibits very high success ratios and outperforms the straightforward method. Table 3 lists the number of successful grasp transfers and grasp assemblies. The first number is the result of our method and the second is the result of the straightforward method. We evaluate 40 stable grasps of the example object for each test.

6.4 Time Complexity

Here, we analyze the time complexity of our algorithm.

Learning Grasp Space: The time spent in the learning stage depends on the number of samples, the time of collision detection, and the time to learn an approximation of configuration space. The collision detection is accelerated using precomputed bounding volume hierarchies of finger links and objects. The time spent stable grasp computation stage depends on the number of particles and the number of iterations. In each iteration, we perform collision detection for each hand configuration and compute its energy function value using Equation 1.

Shape Warping: The time spent on shape warping consists of three stages: rigid alignment computation, correspondence computation, and consistency checking. Its time spent depends on the number of iterations and the time for computing deviations between two objects in each iteration. The correspondence computation and consistency checking depends on the number of points on the objects. We have to compute forward correspondences for all points on the example object and backward correspondences for all points on the novel object.

Replanning: The replanning is an optimization process, depending on the number of iterations and the time complexity of each iteration. In each iteration, we

generate at most 20 samples. We perform collision detection and compute an objective function value for each feasible sample in configuration space.

7 Conclusions, Limitations, and Future Work

In this paper, we considered the problem of object grasping using a multi-fingered robotic hand under the assumption that the 3D models of the objects are known and that the objects have the same topologies and similar geometric shapes. We presented a new approach to grasping a novel object through learning the grasping knowledge of a known object. Our algorithm avoids computing or learning the grasp configurations from scratch. Our experiment shows that our algorithm works for a wide range of object categories. Our method has a high success rate for learning grasps and exhibits a better performance than some previous methods.

Our algorithm has some limitations. First, our algorithm assumes the object-space representation of a complex object is available. Second, it also relies on the object category classification and the quality of segmentation. Fortunately, many model databases [8, 42] have provided a large number of categories and segmented objects. In our future work, we are interested in extending our algorithm to handle partially-known novel models. Moreover, we would like to improve the performance using hardware acceleration so that real-time performance can be achieved.

References

1. J. Aleotti and S. Caselli. Part-based robot grasp planning from human demonstration. In *IEEE International Conference on Robotics and Automation (ICRA)*, pp. 4554–4560. IEEE, 2011.
2. H. B. Amor, O. Kroemer, U. Hillenbrand, G. Neumann, and J. Peters. Generalization of human grasping for multi-fingered robot hands. In *IEEE/RSJ International Conference on Intelligent Robots and Systems*, pp. 2043–2050, 2012.
3. A. Bicchi and V. Kumar. Robotic grasping and contact: A review. In *IEEE International Conference on Robotics and Automation*, vol. 348, p. 353, 2000.
4. I. Biederman. Recognition-by-components: a theory of human image understanding. *Psychological review*, 94(2):115, 1987.
5. J. Bohg, A. Morales, T. Asfour, and D. Kragic. Data-driven grasp synthesis-A survey. *IEEE Transactions on Robotics*, 30(2):289–309, 2014.
6. C. Borst, M. Fischer, and G. Hirzinger. Calculating hand configurations for precision and pinch grasps. In *IEEE/RSJ International Conference on Intelligent Robots and Systems*, vol. 2, pp. 1553–1559, 2002.
7. P. Brook, M. Ciocarlie, and K. Hsiao. Collaborative grasp planning with multiple object representations. In *IEEE International Conference on Robotics and Automation (ICRA)*, pp. 2851–2858, 2011.
8. A. X. Chang, T. Funkhouser, L. Guibas, P. Hanrahan, Q. Huang, Z. Li, S. Savarese, M. Savva, S. Song, H. Su, J. Xiao, L. Yi, and F. Yu. ShapeNet: An Information-Rich 3D Model Repository. Technical Report arXiv:1512.03012 [cs.GR], Stanford University — Princeton University — Toyota Technological Institute at Chicago, 2015.

9. M. Ciocarlie, C. Goldfeder, and P. Allen. Dexterous grasping via eigengrasps: A low-dimensional approach to a high-complexity problem. In *Robotics: Science and Systems Manipulation Workshop*, 2007.
10. M. T. Ciocarlie. Low-dimensional robotic grasping: Eigengrasp subspaces and optimized underactuation. *Ph.D. dissertation, Columbia University, Graduate School of Arts and Sciences*, 2010.
11. M. Clerc and J. Kennedy. The particle swarm - explosion, stability, and convergence in a multidimensional complex space. *IEEE Transactions on Evolutionary Computation*, 6(2):58–73, 2002.
12. N. Curtis and J. Xiao. Efficient and effective grasping of novel objects through learning and adapting a knowledge base. In *IEEE/RSJ International Conference on Intelligent Robots and Systems*, pp. 2252–2257, 2008.
13. R. Diankov. Automated construction of robotic manipulation programs. *Ph.D. dissertation, Carnegie Mellon University, Robotics Institute*, 2010.
14. S. Elkhoury and A. Sahbani. On computing robust n-finger force-closure grasps of 3D objects. *International Conference on Robotics and Automation*, pp. 2480–2486, 2009.
15. C. Ferrari and J. Canny. Planning optimal grasps. In *IEEE International Conference on Robotics and Automation*, pp. 2290–2295, 1992.
16. M. Fischer and G. Hirzinger. Fast planning of precision grasps for 3D objects. *Intelligent Robots and Systems*, 1:120–126, 1997.
17. C. Goldfeder, P. K. Allen, C. Lackner, and R. Pelosof. Grasp planning via decomposition trees. In *IEEE International Conference on Robotics and Automation*, pp. 4679–4684, 2007.
18. C. Goldfeder, M. Ciocarlie, H. Dang, and P. K. Allen. The columbia grasp database. In *IEEE International Conference on Robotics and Automation*, pp. 1710–1716, 2009.
19. U. Hillenbrand. Non-parametric 3d shape warping. In *IEEE International Conference on Pattern Recognition*, pp. 2656–2659, 2010.
20. U. Hillenbrand and M. A. Roa. Transferring functional grasps through contact warping and local replanning. In *IEEE/RSJ International Conference on Intelligent Robots and Systems (IROS)*, pp. 2963–2970, 2012.
21. D. D. Hoffman and W. A. Richards. Parts of recognition. *Cognition*, 18(1-3):65–96, 1984.
22. K. Huebner, S. Ruthotto, and D. Kragic. Minimum volume bounding box decomposition for shape approximation in robot grasping. In *IEEE International Conference on Robotics and Automation*, pp. 1628–1633, 2008.
23. S. Kirkpatrick, C. D. Gelatt, and M. P. Vecchi. Optimization by simulated annealing. *science*, 220(4598):671–680, 1983.
24. M. Kopicki, R. Detry, F. Schmidt, C. Borst, R. Stolkin, and J. L. Wyatt. Learning dexterous grasps that generalise to novel objects by combining hand and contact models. In *IEEE International Conference on Robotics and Automation*, pp. 5358–5365, 2014.
25. S. Levine, P. Pastor, A. Krizhevsky, J. Ibarz, and D. Quillen. Learning hand-eye coordination for robotic grasping with deep learning and large-scale data collection. *The International Journal of Robotics Research*, 37(4-5):421–436, 2018.
26. Y. Li, J. L. Fu, and N. S. Pollard. Data-driven grasp synthesis using shape matching and task-based pruning. *IEEE Transactions on Visualization and Computer Graphics*, 13(4):732–747, 2007.

27. M. Madry, D. Song, and D. Kragic. From object categories to grasp transfer using probabilistic reasoning. In *IEEE International Conference on Robotics and Automation*, pp. 1716–1723, 2012.
28. J. Mahler, J. Liang, S. Niyaz, M. Laskey, R. Doan, X. Liu, J. A. Ojea, and K. Goldberg. Dex-net 2.0: Deep learning to plan robust grasps with synthetic point clouds and analytic grasp metrics. *arXiv preprint arXiv:1703.09312*, 2017.
29. J. Mahler, F. T. Pokorny, B. Hou, M. Roderick, M. Laskey, M. Aubry, K. Kohlhoff, T. Kröger, J. Kuffner, and K. Goldberg. Dex-net 1.0: A cloud-based network of 3d objects for robust grasp planning using a multi-armed bandit model with correlated rewards. In *Robotics and Automation (ICRA), 2016 IEEE International Conference on*, pp. 1957–1964. IEEE, 2016.
30. X. Markenscoff and C. H. Papadimitriou. Optimum grip of a polygon. *International Journal of Robotics Research*, 8(2):17–29, 1989.
31. Z. C. Marton, R. B. Rusu, D. Jain, U. Klank, and M. Beetz. Probabilistic categorization of kitchen objects in table settings with a composite sensor. In *IEEE/RSJ International Conference on Intelligent Robots and Systems*, pp. 4777–4784, 2009.
32. A. T. Miller and P. K. Allen. GraspIt! A versatile simulator for robotic grasping. *IEEE Robotics & Automation Magazine*, 11(4):110–122, 2004.
33. E. Nikandrova and V. Kyrki. Category-based task specific grasping. *Robotics and Autonomous Systems*, 70:25–35, 2015.
34. R. Pelossof, A. T. Miller, P. K. Allen, and T. Jebara. An SVM learning approach to robotic grasping. *Proceedings of the IEEE International Conference on Robotics and Automation*, 4:3512–3518, 2004.
35. F. T. Pokorny and D. Kragic. Classical grasp quality evaluation: New algorithms and theory. In *IEEE/RSJ Intelligent Robots and Systems*, 2013.
36. S. Redon, M. C. Lin, D. Manocha, and Y. J. Kim. Fast continuous collision detection for articulated models. *Journal of Computing and Information Science in Engineering*, 5(2):126–137, 2005.
37. D. Rodriguez and S. Behnke. Transferring category-based functional grasping skills by latent space non-rigid registration. *IEEE Robotics and Automation Letters*, 3(3):2662–2669, 2018.
38. D. Rodriguez, C. Cogswell, S. Koo, and S. Behnke. Transferring grasping skills to novel instances by latent space non-rigid registration. In *IEEE International Conference on Robotics and Automation*, 2018.
39. L. Shapira, A. Shamir, and D. Cohen-Or. Consistent mesh partitioning and skeletonisation using the shape diameter function. *The Visual Computer*, 24(4):249, 2008.
40. T. Stouraitis, U. Hillenbrand, and M. A. Roa. Functional power grasps transferred through warping and replanning. In *IEEE International Conference on Robotics and Automation*, pp. 4933–4940, 2015.
41. N. Vahrenkamp, L. Westkamp, N. Yamanobe, E. E. Aksoy, and T. Asfour. Part-based grasp planning for familiar objects. In *IEEE-RAS 16th International Conference on Humanoid Robots (Humanoids)*, pp. 919–925, 2016.
42. W. Wohlkinger, A. Aldoma, R. B. Rusu, and M. Vincze. 3dnet: Large-scale object class recognition from cad models. In *ICRA*, pp. 5384–5391, 2012.
43. F. Zacharias, C. Borst, and G. Hirzinger. Object-specific grasp maps for use in planning manipulation actions. *Advances in Robotics Research*, pp. 203–214, 2009.

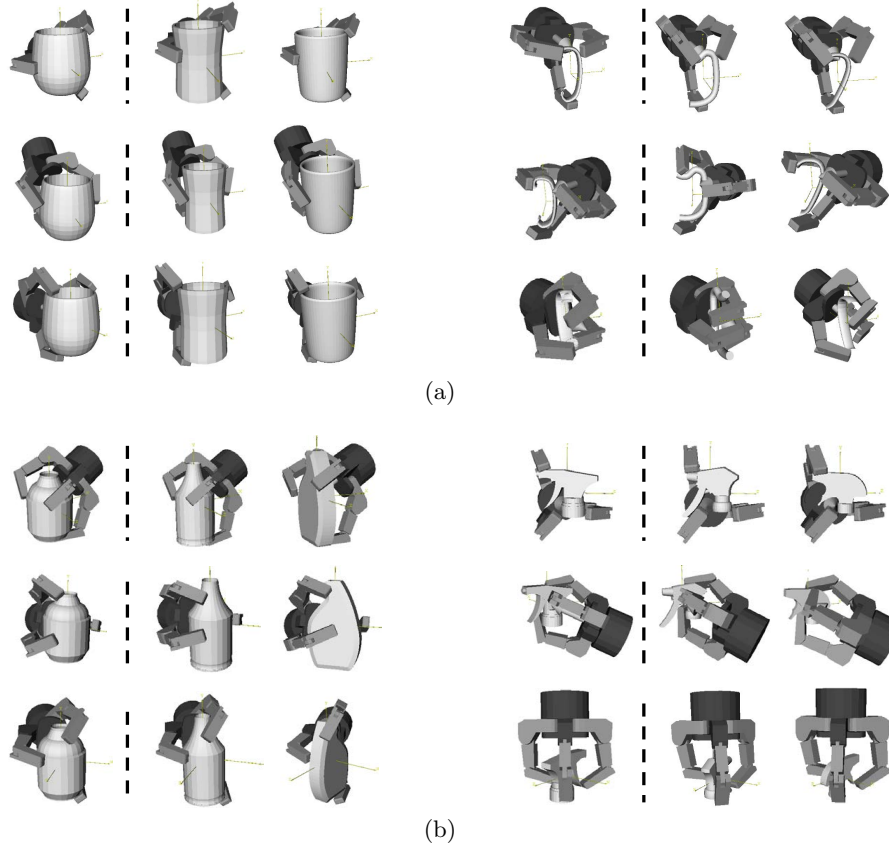


Fig. 5. Generating stable grasps using local replanning. The left three columns and the right three columns show results of different parts. The column on the left side of the dashed line shows stable grasps for each part of known example objects. The two columns on the right side of the dashed line are the resulting transferred grasps for novel objects.

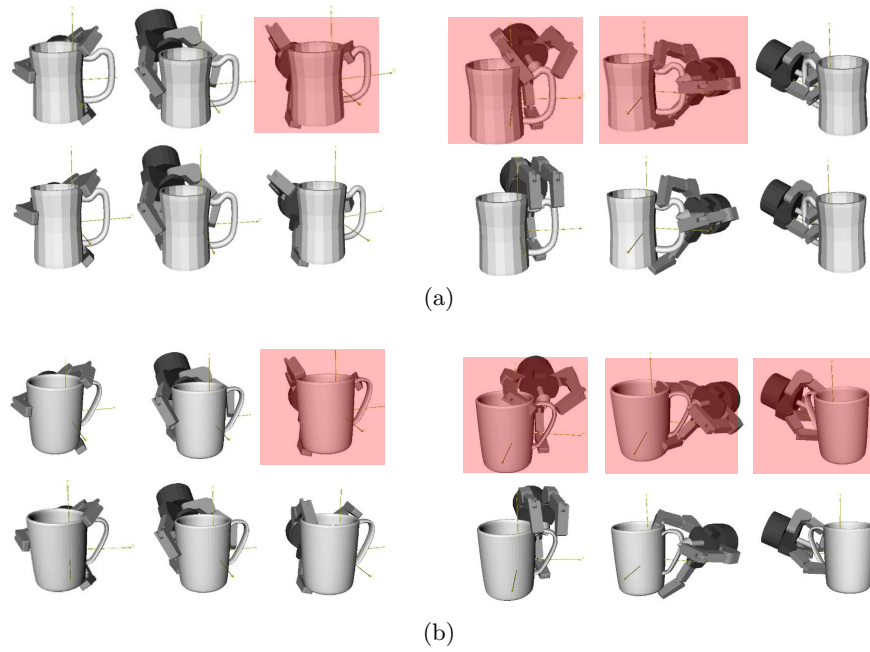


Fig. 6. Grasp configurations of novel objects before and after part assembly and local replanning. The upper row shows the assembly grasps without replanning; some grasps (highlighted in red) cause collisions with other object parts. We use local planning to compute a feasible and stable grasp, as shown in the bottom row.

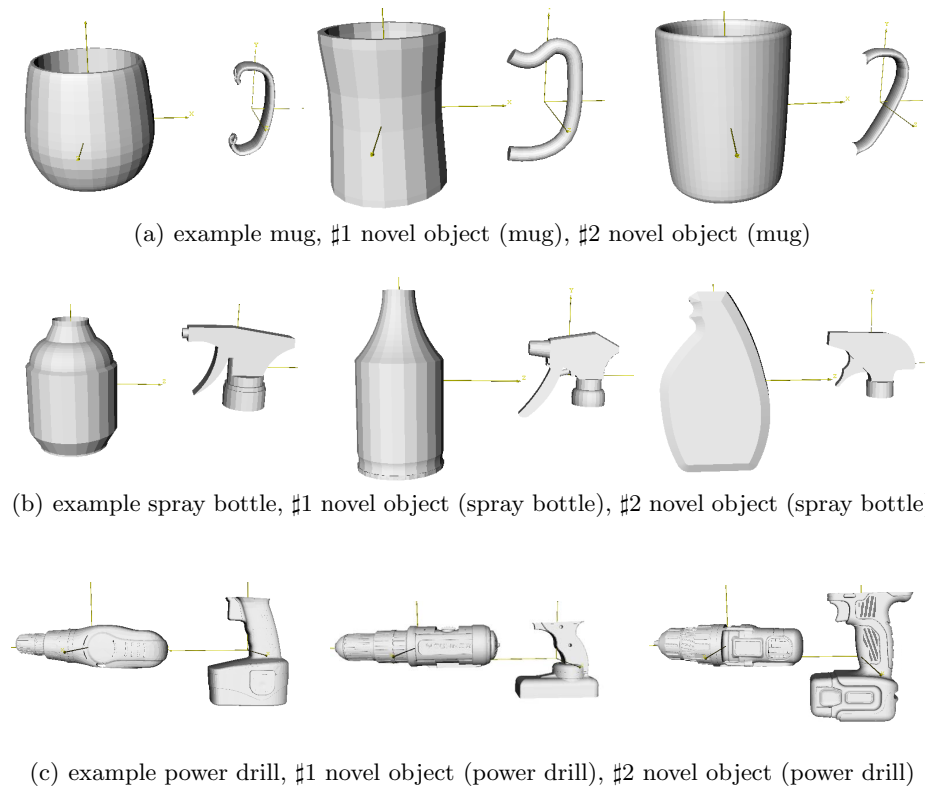


Fig. 7. Our experiments use three categories of objects and their segmentations. (a) mug; (b) spray bottle; (c) power drill. The objects in the first column are known examples and the others are novel objects.

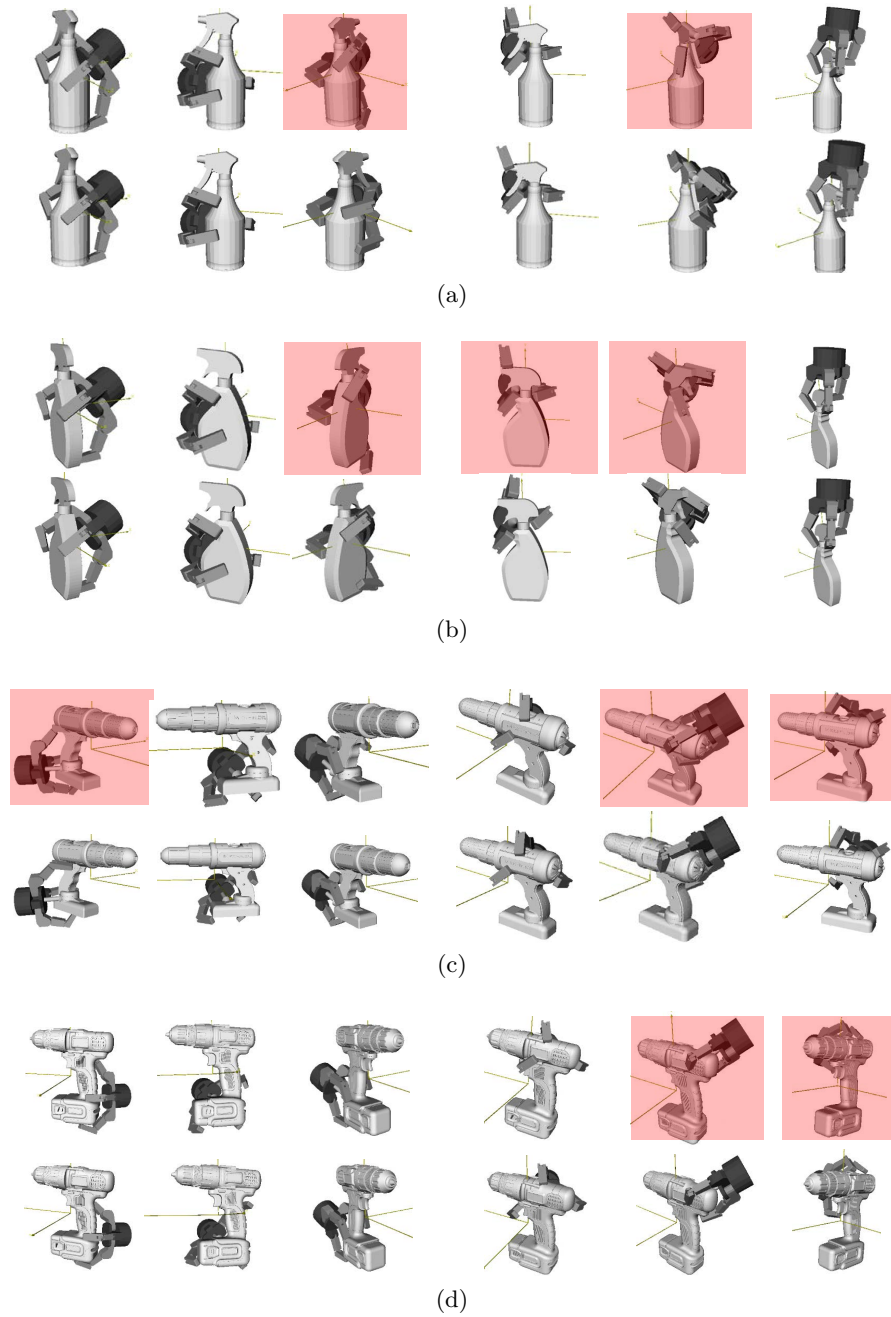


Fig. 8. Grasp configurations for novel objects after part assembly and local replanning. Some grasps (highlighted in red) cause collisions with other object parts. Local replanning is able to find a feasible and stable grasp, as shown in the row below.

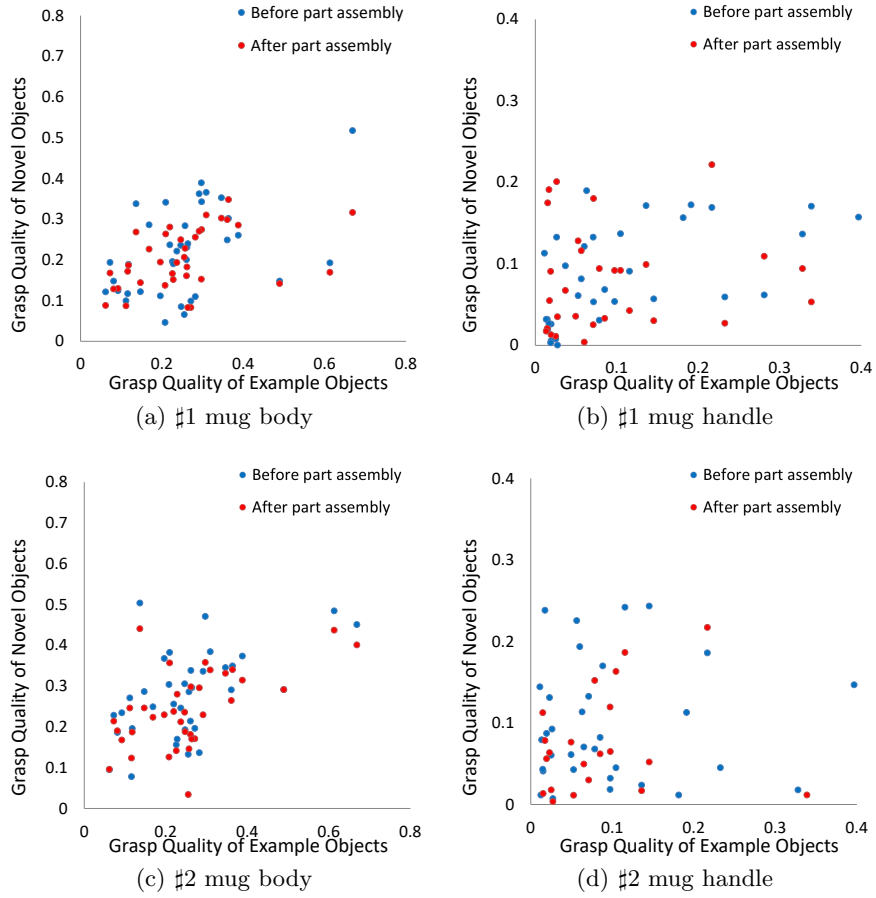


Fig. 9. Grasp quality before and after part assembly and replanning. (a)(b) mug model #1; (c)(d) mug model #2.

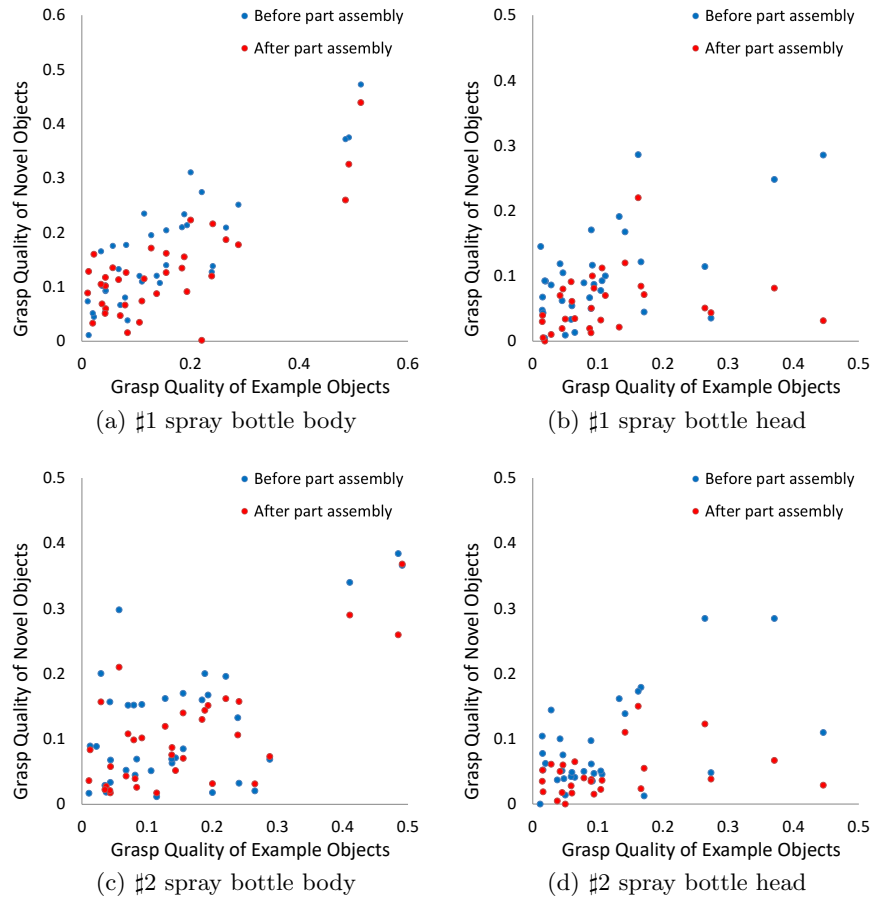


Fig. 10. Grasp quality before and after part assembly and replanning. (a)(b) spray bottle model #1; (c)(d) spray bottle model #2.

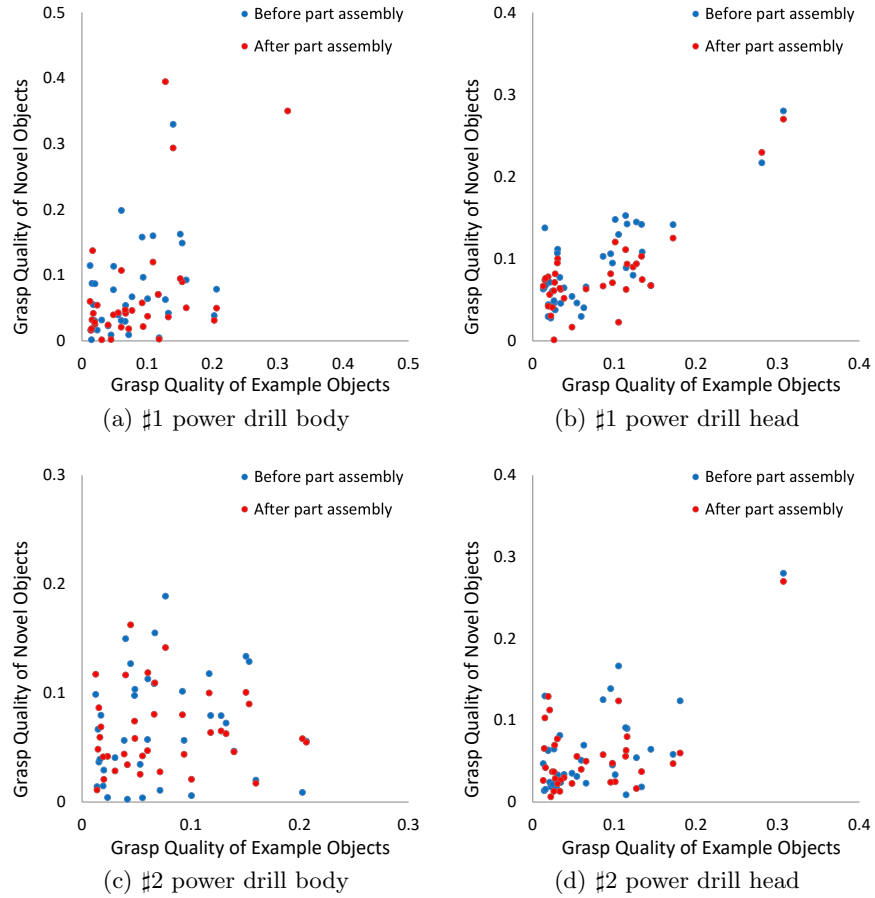


Fig. 11. Grasp quality before and after part assembly and replanning. (a)(b) power drill model #1; (c)(d) power drill model #2.

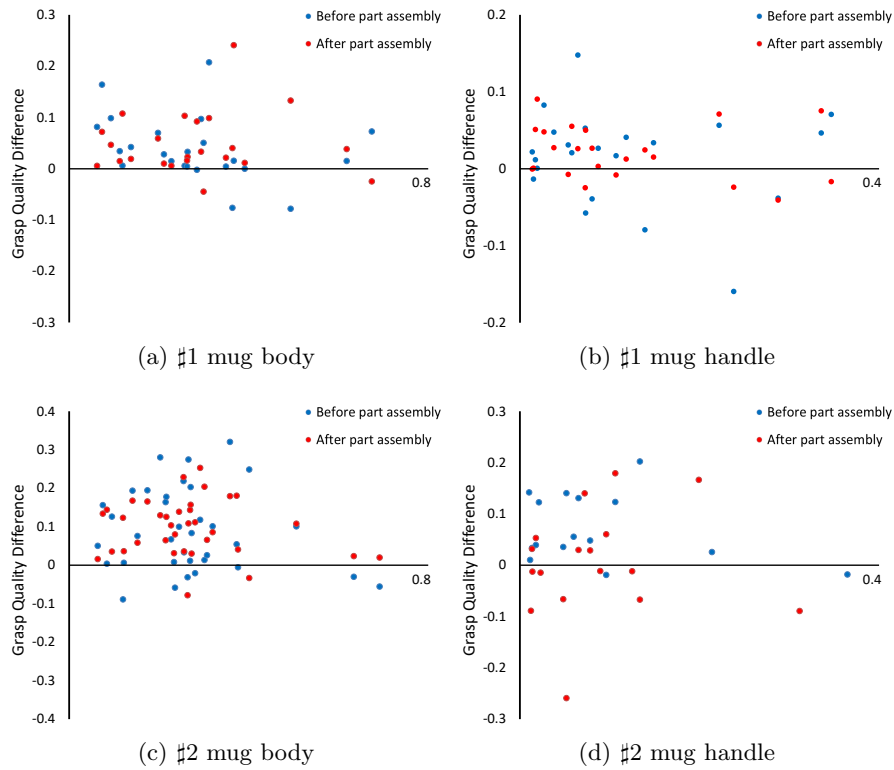


Fig. 12. Grasp quality comparison between our method and a straightforward method (straightening the colliding fingers and enclosing the object). The points distribute above horizontal axes mean our method outperform the straightforward method. (a)(b) mug model #1; (c)(d) mug model #2.

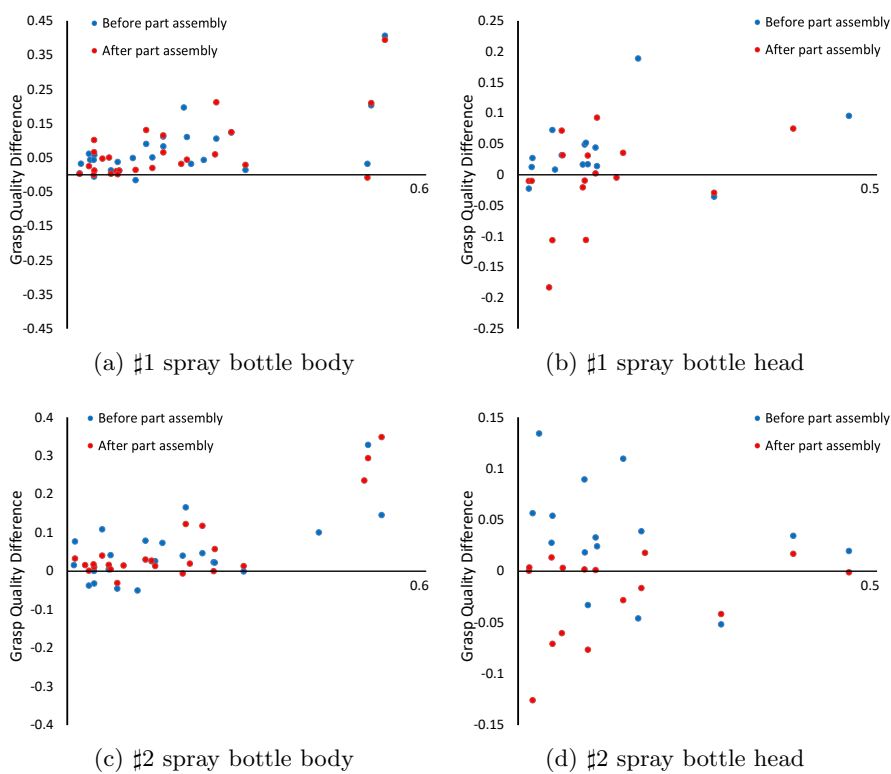


Fig. 13. Grasp quality comparison between our method and a straightforward method (straightening the colliding fingers and enclosing the object). The points distribute above horizontal axes mean our method outperform the straightforward method. (a)(b) spray bottle model #1; (c)(d) spray bottle model #2.

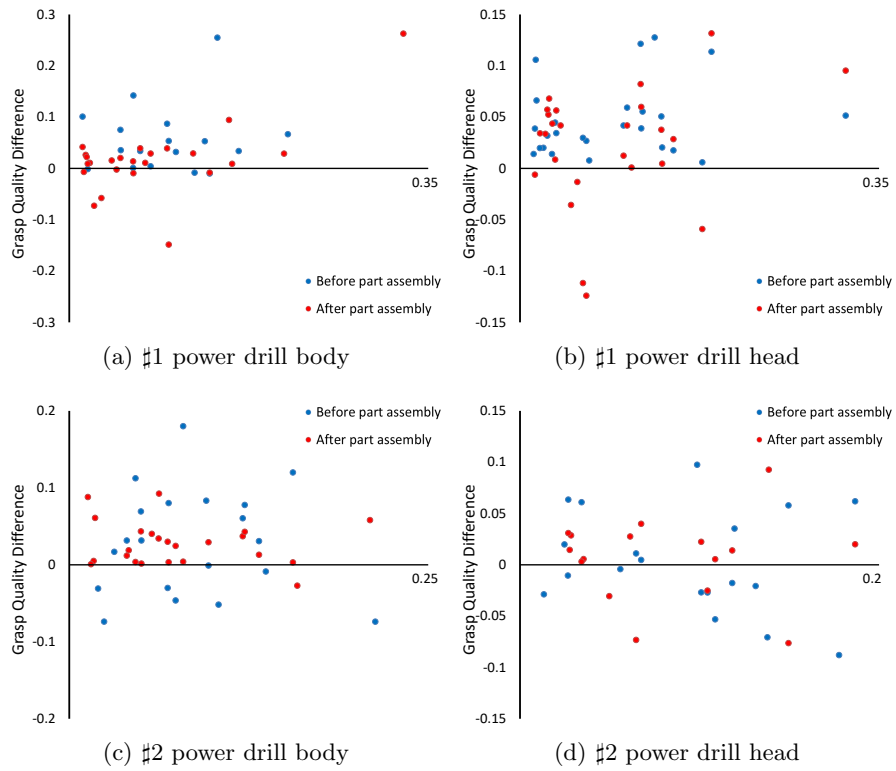


Fig. 14. Grasp quality comparison between our method and a straightforward method (straightening the colliding fingers and enclosing the object). (a)(b) power drill model #1; (c)(d) power drill model #2.